Numerical simulation of roll waves in pipelines using the two-fluid model

Sanderse, B.; Misra, S.; Dubinkina, S.; Henkes, R. A.W.M.; Oosterlee, C. W.

Publication date
2018

Document Version
Final published version

Published in
Proceedings 11th North American Conference on Multiphase Technology

Numerical simulation of roll waves in pipelines using the two-fluid model

B Sanderse [1], S Misra [1,2], S Dubinkina [1], R A W M Henkes [2,3], C W Oosterlee [1,2]
[1] Centrum Wiskunde & Informatica, Amsterdam, The Netherlands
[2] Delft University of Technology, The Netherlands
[3] Shell Technology Centre Amsterdam, The Netherlands

A finite volume discretization of the incompressible two-fluid model in four-equation form is proposed for simulating roll waves appearing in multiphase pipelines. The new formulation has two important advantages compared to existing roll wave simulators: (i) it is conservative by construction, meaning that the correct shock magnitude is obtained at the hydraulic jump, and (ii) it can be more easily extended with additional physics (e.g. compressibility, axial diffusion, surface tension), without rederiving the model equations.

A simple, robust, first-order upwind discretization of the four-equation model is able to capture the roll wave profiles, although a fine grid is needed to achieve converged results. The four-equation model leads to new roll wave solutions that differ from existing analytical and numerical results. Our solutions are believed to be physically more correct because the shock relations satisfy physically conserved quantities.

1 INTRODUCTION

The design and maintenance of flow assurance systems involves complex multiphase flow through pipelines. The behaviour of this multiphase flow can take many forms (flow regimes), depending on parameters like flow rates, fluid properties and pipeline properties. An important flow regime is slug flow, in which liquid pockets, separated by gas bubbles, propagate in an alternating fashion with high speed along the pipeline. These slugs can have a large influence on the system design, such as required support (to handle the induced bend forces, vibrations, fatigue) and the size of the separator and liquid drain rate capacity. In order to assure adequate system design and continued operation, numerical simulations play an important role. Many numerical simulations are based on the one-dimensional two-fluid model, examples are the engineering design tools such as OLGA or LedaFlow [4,14]. However, the conventional two-fluid model has an issue of conditional well-posedness: under certain conditions, grid refinement does not yield unique solutions. A significant amount of scientific effort has been devoted towards resolving this issue, for example by inclusion of surface tension, artificial diffusion, virtual mass, momentum flux parameters, and a separate pressure for each phase. However, a fully satisfactory solution that results in grid-independent slug capturing results is still missing.

In this work, instead of studying directly slug flow, we assess the capabilities of the two-fluid model in capturing a travelling-wave surface instability named *roll waves*. Although roll waves are not as vigorous as slugs, the availability of analytical solutions yields the possibility to study the issues of well-posedness and stability of the two-fluid model in detail; understanding roll waves thus forms an important step towards performing accurate and reliable slug capturing with the two-fluid model.

Roll wave modelling and simulation attempts are not new, and the theoretical foundations were laid down firstly by Dressler [7] for shallow water equations and then by Watson [23] using the two-fluid model for flow in pipelines. Johnson [12] performed an experimental study of roll waves and compared these with an analytical model similar to Watson. Numerical simulations of roll waves based on solving the two-fluid model equations are relatively scarce - recent studies are the ones of Akselsen [2] and Holmås [9]. Akselsen uses a two-equation formulation of the two-fluid model and shows that properly designed characteristics methods outperform a finite volume method with a Roe scheme, when comparing to an analytical roll wave solution. Holmås uses the same two-equation formulation which he solves with a pseudo-spectral method. His results compare relatively well with the experiments of Johnson [12] and roll waves are obtained for a relatively wide selection of initial conditions.

There are however two issues related to these approaches to roll wave modelling and simulation. Firstly, the reformulation of the equations into a two-equation model is strictly not valid when discontinuous solutions (such as roll waves) are present, leading to a difference in jump conditions between the four-equation model and the two-equation model. This was also noted by both Watson [23] and Akselsen [1]. Secondly, in practice many multiphase flow pipeline simulators (both commercial [4,14] as well as academic codes [11,8]) do not employ purpose-made numerical schemes such as the characteristics methods by Akselsen [2] or the pseudospectral method by Holmås [9]. Instead, the `standard' conservative four-equation model is used, which is discretized with an upwind-type spatial discretization method. This four-equation model is more amenable for extension with additional physics, such as compressibility, dispersion and entrainment of bubbles and droplets, temperature effects, etc.

Two open questions are therefore: (i) is the two-fluid model in the standard (four-equation) form, discretized with an upwind-based finite volume method, able to capture roll wave solutions, and (ii) do these solutions differ from the roll wave solutions of the two-equation model. These are the questions that we will answer in this work.

The paper outline is as follows. In section 2 the governing equations of the two-fluid model and the recipe for constructing analytical roll wave solutions are given. In section 3 our numerical method in terms of spatial and temporal discretization is described. Section 4 shows numerical roll wave solutions based on the test case parameters of Johnson [12] and Akselsen [2], including a comparison with analytically obtained solutions. Finally, in section 5 conclusions and directions for future work are given.

2 GOVERNING EQUATIONS AND ROLL WAVES

2.1 The two-fluid model

The two-fluid model can be derived by considering the stratified flow of liquid and gas in a pipeline (for a recent discussion of the two-fluid model, see for example [18]). The main assumptions that we make are that the flow is one-dimensional, incompressible, stratified, and isothermal. Transverse pressure variation is introduced via level gradient terms. Surface tension is neglected. This leads to the following equations for conservation of mass and momentum of each phase:

$$\frac{\partial}{\partial t}\left(\rho_g A_g\right)+\frac{\partial}{\partial s}\left(\rho_g u_g A_g\right) = 0, \tag{1}$$

$$\frac{\partial}{\partial t}\left(\rho_l A_l\right)+\frac{\partial}{\partial s}\left(\rho_l u_l A_l\right)=0, \tag{2}$$

$$\frac{\partial}{\partial t}\left(\rho_g u_g A_g\right)+\frac{\partial}{\partial s}(\rho_g u_g^2 A_g) = -\frac{\partial p}{\partial s}A_g + LG_g + \underbrace{-\tau_{gl}P_{gl} - \tau_g P_g - \rho_g A_g g_s + F_{\text{body}} A_g}_{S_g}, \tag{3}$$

$$\frac{\partial}{\partial t}\left(\rho_l u_l A_l\right)+\frac{\partial}{\partial s}(\rho_l u_l^2 A_l) = -\frac{\partial p}{\partial s}A_l + LG_l + \underbrace{\tau_{gl}P_{gl} - \tau_l P_l - \rho_l A_l g_s + F_{\text{body}} A_l}_{S_l}, \tag{4}$$

supplemented with the volume constraint equation,

$$A_g + A_l = A. \tag{5}$$

In these equations the subscript denotes either gas *(g)* or liquid *(l)*. The model features four evolution equations, one constraint equation, and five unknowns (A_g, A_l, u_g, u_l, p), which are a function of the independent variables s (coordinate along the pipeline axis) and t (time). ρ denotes the density (assumed constant), A the cross-sectional area of the pipe, A_g, and A_l (also referred to as the hold-ups) the cross-sectional areas occupied by the gas or liquid, R the pipe radius, h the height of the liquid layer measured from the bottom of the pipe, u the phase velocity, p the pressure at the interface, τ the shear stress (with the wall or at the interface), g the gravitational constant, φ the local inclination of the pipeline with respect to the horizontal, such that $g_n = g\cos\varphi$ and $g_s = g\sin\varphi$.

The level gradient terms LG are given by [20]:

$$LG_g = \frac{\partial HG_g}{\partial s}, \quad HG_g = \rho_g g_n\left[(R-h)A_g + \frac{1}{12}P_{gl}^3\right], \tag{6}$$

$$LG_l = \frac{\partial HG_l}{\partial s}, \quad HG_l = \rho_l g_n\left[(R-h)A_l - \frac{1}{12}P_{gl}^3\right]. \tag{7}$$

For incompressible flow these expressions simplify to $LG_g = -\rho_g g_n A_g \frac{\partial h}{\partial s}$, $LG_l = -\rho_l g_n A_l \frac{\partial h}{\partial s}$, but we stick to the form displayed in equations (6)-(7) because this form is conservative. A_l and h are related by a non-linear algebraic expression. The wetted and interfacial perimeters P_g, P_l and P_{gl} can similarly be expressed in terms of the hold-up A_l or the interface height h (see [20]).

The driving pressure force $F_{\text{body}} = -\frac{dp_{\text{body}}}{ds}$ in the gas and liquid momentum equations is required for our simulations because they involve periodic boundary conditions. As friction model we use the Biberg friction model, see [6, 10, 1], which provides (implicit) expressions for τ_g, τ_l and τ_{gl}. The Biberg model is based on turbulent interaction between the two-phases. The flow in both the fluids is governed by an algebraic eddy viscosity distribution from which analytical velocity distributions are derived, which in turn leads to a consistent set of wall and interfacial friction formulas. Compared to a 'standard' friction

model, in which the interfacial friction factor is expressed as a multiple of the gas friction factor (see e.g. [12, 10]), the Biberg model acts as an additional means of stabilization, especially for higher hold-up levels [10].

Initial and boundary conditions determine whether the equations form a well-posed initial boundary value problem. It is well-known that, depending on the velocity difference between the phases, the two-fluid model equations can become ill-posed [3, 19, 22]. In this paper we restrict ourselves to test cases for which the model is well-posed. Additionally, the initial conditions will determine whether disturbances will grow (unstable) or damp in time (stable). For roll wave simulation such an unstable mode will be used to trigger wave growth that leads to shock formation.

2.2 Two-equation model

The roll wave simulations of Holmås [10] and Akselsen [2] are based on a two-equation reformulation of the incompressible two-fluid model equations (1)-(5). The first equation is typically the liquid hold-up equation in incompressible form,

$$\frac{\partial}{\partial t}\left(A_l\right)+\frac{\partial}{\partial s}\left(u_l A_l\right)=0. \tag{8}$$

The second equation is an equation for the difference in momenta, in which the pressure has been eliminated:

$$\frac{\partial}{\partial t}\left(\rho_l u_l-\rho_g u_g\right)+\frac{\partial}{\partial s}\left(\frac{1}{2}\left(\rho_l u_l^2-\rho_g u_g^2\right)\right)=-(\rho_l-\rho_g)g_n\frac{\partial h}{\partial s}+\frac{S_l}{A_l}-\frac{S_g}{A_g}. \tag{9}$$

The system is closed with the volume constraint (5) and the volumetric flow constraint

$$A_g u_g + A_l u_l = Q(t), \tag{10}$$

where $Q(t)$ is the total volumetric flow rate. We note that this 'pressure-free' two-equation model is only equivalent to the four-equation two-fluid model for sufficiently smooth solutions. In case shock waves appear in the solution, as is the case for roll waves, the pressure-free model is not equivalent [1, 15] and should in principle not be used. Although the difference between the conservative and non-conservative system is small in the case of weak shocks [23, 1], we consider the four-equation model to be the most physically sound model and it will therefore be used in our numerical simulations.

2.3 Analytical roll wave model

Roll waves are specific travelling-wave analytical solutions of the incompressible two-fluid model, which feature a transition from supercritical to subcritical flow through a discontinuity (a hydraulic jump). A demonstrative roll wave profile is presented in figure 1.

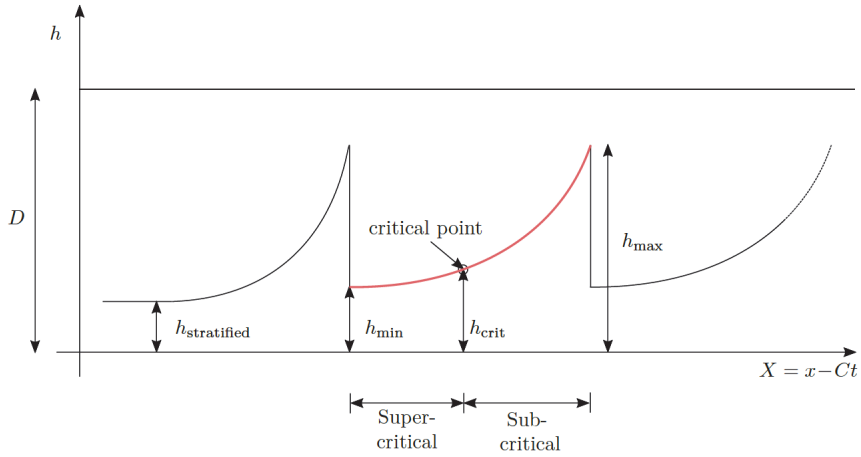

Figure 1: Schematic of a roll wave profile in the moving reference frame.

Watson derived a procedure for obtaining analytical roll wave solutions for the incompressible two-fluid model [23], which we shortly summarize here. The main step is to transform the partial differential equations (1)-(4) into an ordinary differential equation (ODE) describing the interface, by applying the coordinate transformation

$$X = x - Ct, \tag{11}$$

assuming that waves exist travelling with a constant wave speed C. After the coordinate transformation the mass balance equations can be integrated directly to yield

$$A_g\left(u_g - C\right) = K_g \quad \text{and} \quad A_l\left(u_l - C\right) = K_l, \tag{12}$$

where Kg and Kl are constants, namely the progressive discharge rate of gas and liquid respectively. The momentum balance equations reduce to a single ODE for the liquid hold-up h:

$$\frac{dh}{dX} = \frac{E}{D}, \tag{13}$$

where

$$E = H\left(\frac{S_l}{A_l} - \frac{S_g}{A_g}\right), \tag{14}$$

$$D = \left(\rho_l - \rho_g\right) g_n H - \rho_l \left(u_l - C\right)^2 - \rho_g \frac{A_l}{A_g}\left(u_g - C\right)^2, \tag{15}$$

$$H = \frac{A_l}{\left(\frac{dA_l}{dh}\right)} = \frac{A_l}{P_{lg}}. \tag{16}$$

When the flow transitions from subcritical to supercritical it goes smoothly through the critical point h_{crit} at which E and D should have a common root. On the other hand, the flow transition from supercritical to subcritical is accomplished through a hydraulic jump.

The jump condition follows by integrating equation (9) over an infinitesimally small volume

$$\left[\left(\rho_l-\rho_g\right)g_n h-\frac{1}{2}\rho_l\frac{K_l^{\,2}}{A_l^{\,2}}-\frac{1}{2}\rho_g\frac{K_g^{\,2}}{A_g^{\,2}}\right]_{h_{\min}}^{h_{\max}}=0. \tag{17}$$

Note again, that this shock condition is not a momentum conserving condition. Instead it conserves a difference in the momentum of two phases.

3 NUMERICAL METHOD

3.1 Spatial discretization

The spatial discretization is on a staggered grid, consisting of N 'pressure' and $N+1$ 'velocity' volumes. The midpoints of the velocity volumes lie on the faces of the pressure volumes, as indicated in figure 2. The pressure, density, hold-up and mass are defined in the centre of the pressure volumes, whereas the velocity and momentum are defined in the centre of the velocity volumes. For details we refer to [20, 21]. The unknowns are given by the vector of conservative variables $U(t)$:

$$U(t)=\begin{pmatrix} m_g \\ m_l \\ I_g \\ I_l \end{pmatrix}=\begin{pmatrix} [(\rho_g A_g)_1\ldots(\rho_g A_g)_N]^T \\ [(\rho_l A_l)_1\ldots(\rho_l A_l)_N]^T \\ [(\rho_g A_g u_g)_{1/2}\ldots(\rho_g A_g u_g)_{N+1/2}]^T \\ [(\rho_l A_l u_l)_{1/2}\ldots(\rho_l A_l u_l)_{N+1/2}]^T \end{pmatrix}, \tag{18}$$

and the pressure:

$$p(t)=[p_1\ldots p_N]^T. \tag{19}$$

Note that m_g, m_l, I_g and I_l, are vectors, containing mass and momentum (per unit pipe length) at the pressure and velocity volumes, respectively. $U(t)$ and $p(t)$ are both a function of time only.

We start with conservation of mass for phase β (β is liquid or gas). Integration of equation (2) in s-direction over a pressure volume gives:

$$\frac{\mathrm{d}}{\mathrm{d}t}\left(m_{\beta,i}\Delta s_i\right)+I_{\beta,i+1/2}-I_{\beta,i-1/2}=0, \tag{20}$$

where the convective fluxes can be directly expressed in terms of the momenta I at the staggered locations, so no approximation is involved in this term.

For conservation of momentum we proceed in a similar way. Integration of (4) in s-direction over a velocity volume gives:

$$\frac{\mathrm{d}}{\mathrm{d}t}\left(I_{\beta,i+1/2}\Delta s_{i+1/2}\right)+\left(\rho_\beta A_\beta\right)_{i+1}(u_{\beta,i+1})^2-\left(\rho_\beta A_\beta\right)_i(u_{\beta,i})^2=-A_{\beta,i+1/2}\left(p_{i+1}-p_i\right)+\mathrm{LG}_{\beta,i+1/2}+S_{\beta,i+1/2}\Delta s_{i+1/2}. \tag{21}$$

and the level gradient terms for the gas and liquid are given by (+ for gas, - for liquid)

$$\mathrm{LG}_{\beta,i+1/2} = \rho_\beta g_n \left(\left((R-h)A_\beta \pm \frac{1}{12} P_{gl}^3 \right)_i - \left((R-h)A_\beta \pm \frac{1}{12} P_{gl}^3 \right)_{i-1} \right). \quad (22)$$

The convective terms in (21) are given by a first order upwind scheme, e.g. $u_{i+1} = u_{i+1/2}$ when $u_{i+1/2} > 0$. The system is closed with the volume constraint (5).

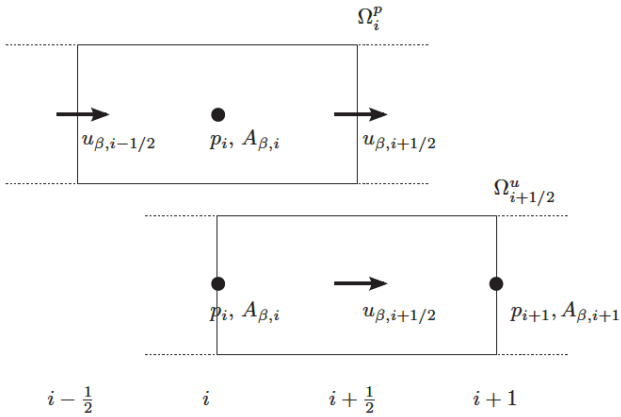

Figure 2: Staggered grid layout.

3.2 Temporal discretization

The temporal discretization of the semi-discrete equations arising after spatial discretization is performed with the half-explicit Runge-Kutta method described in [21]. This method is explicit for the mass and momentum equations and implicit for the volume constraint equation, which is solved via a pressure Poisson equation. In the simulations in this work the RK4 method from [21] is used, which is fourth order accurate for all variables (hold-up fraction, phase velocities, pressure), and requires a CFL-type time-step restriction based on the eigenvalues of the two-fluid model. The fourth order accurate scheme makes the temporal discretization error negligible compared to the spatial discretization error.

4 ROLL WAVE SIMULATION RESULTS

4.1 Test case description and flow pattern map

An important database with experimentally observed roll waves has been provided in the work of Johnson [12, 13]. His experiments concerned the stratified flow of water and SF_6 at the IFE lab in Kjeller, Norway. The test case parameters from his set-up are shown in table 1. These test case parameters are also used in the works of Holmås [10, 9] and Akselsen [2]. Holmås [9] does not make a comparison with analytical roll wave solutions, but concentrates on the comparison with the experimental data of Johnson. Akselsen [2] on the other hand does not perform a comparison with experimental data but focuses solely on the convergence of the characteristics methods towards the analytical solution upon grid refinement. In our test case we follow the approach of Akselsen, i.e. comparison with the analytical solution.

Table 1: Parameter values for experimental roll wave investigation used by Johnson [13].

parameter	value	unit
ρ_l	998	kg/m^3
ρ_g	50	kg/m^3
R	0.05	m
μ_g	1.61 10^{-5}	Pa s
μ_l	9.98 10^{-3}	Pa s
φ	0, 0.1, 0.25, 1, 2.5, 5	deg
ϵ	2 10^{-5}	m

We concentrate on the case of $\varphi = 1^\circ$. A flow pattern map is constructed by performing a viscous Kelvin-Helmholtz analysis and drawing the neutral stability line. Figure 3 shows the resulting stable and unstable regions, which is similar to the one presented in Holmås [10]. We note that the neutral stability line of the 'standard' interfacial friction model $f_i = f_g$ as mentioned by Holmås is not visible in this figure - it appears at much lower superficial velocities than the ones considered in this figure. Analytical roll wave solutions could not be constructed for this condition. Similarly, for the interfacial stress model considered in Liao et al. [17] (namely $f_i = \max(f_g, 0.014)$), no roll waves exist because the considered initial conditions for the dynamic simulation (as indicated by the open symbol in figure 3) within the VKH stability boundary (given by the dashed line in figure 3). With the Biberg friction model, roll waves can be simulated, as the considered conditions lie just outside the VKH stability curve (the solid line in figure 3).

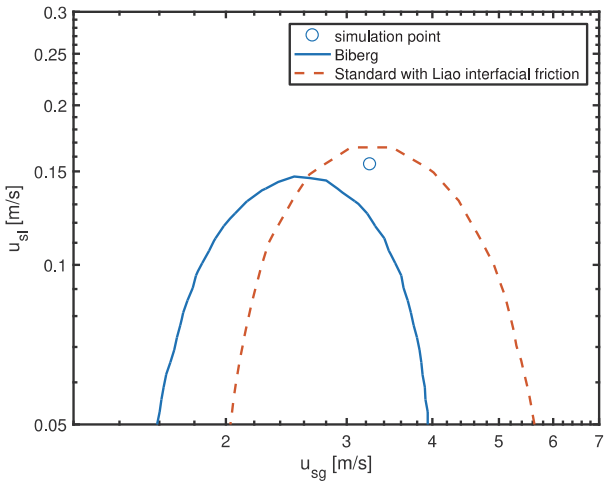

Figure 3: Flow pattern map for $\varphi = 1^\circ$ (a similar graph is in Holmås, figure 2-c [10]. Dashed line is when simulating with the standard model with $f_i = \max(f_g, 0.014)$. The standard model with $f_i = f_g$ is unstable for this range of conditions.

4.2 Comparison numerical and analytical roll waves

We will now compare numerically generated roll waves with analytical solutions. As initial condition we take the flow rate and hold-up value from Akselsen [2]: Q_{tot}/A = 3.4 m/s,

$\overline{h}_l / D = 0.2$. Solving the steady-state momentum equation *E=0* yields the following initial superficial velocities and driving pressure gradient:

$$u_{sg} \approx 3.245 \text{ m/s}, \tag{23}$$

$$u_{sl} \approx 0.155 \text{ m/s}, \tag{24}$$

$$F_{\text{body}} = \frac{dp_{\text{body}}}{dx} \approx -124.997 \text{ Pa/m}. \tag{25}$$

This case is shown on the flow pattern map in figure 3. At these superficial velocities, the analytical roll wave solution with a (pre-set) roll wave length $\lambda = 3\text{m}$ is given by [2]:

$$C \approx 1.4408\text{m/s}, \tag{26}$$

$$\Delta h = h_{\max} - h_{\min} \approx 0.0996 D = 0.00996 \text{ m}. \tag{27}$$

To numerically simulate these roll waves, we take a domain of length $L = \lambda$ with periodic boundary conditions and discretize the domain in N = 80, 160, 320, 640 and 1280 grid points. The number of grid points per diameter, $D / \Delta s$, is approximately 2.5, 5, 10, 20 and 40 respectively. Note that for N = 40 no roll wave solution was found (the initial wave damped out). A period of 200 seconds is simulated, corresponding to approximately 150 wave revolutions, indicating an equivalent pipeline of length of 450 m. For the two finest grids 100 seconds are simulated. A time step of $\Delta t = (2/3)L/N$ is used, which corresponds roughly to a CFL number of 1 based on the largest maximum eigenvalue (which is around 1.5 m/s). The initial condition is a single wave with a hold-up amplitude of 0.01, wave number $k = 2\pi / L$ and angular frequency chosen such that a single, unstable, wave is triggered [20].

An example of the roll wave shape at different time instances is shown in figure 4 in terms of the hold-up and the pressure (after t = 100 s the shape remains virtually unchanged, see also figure 6).

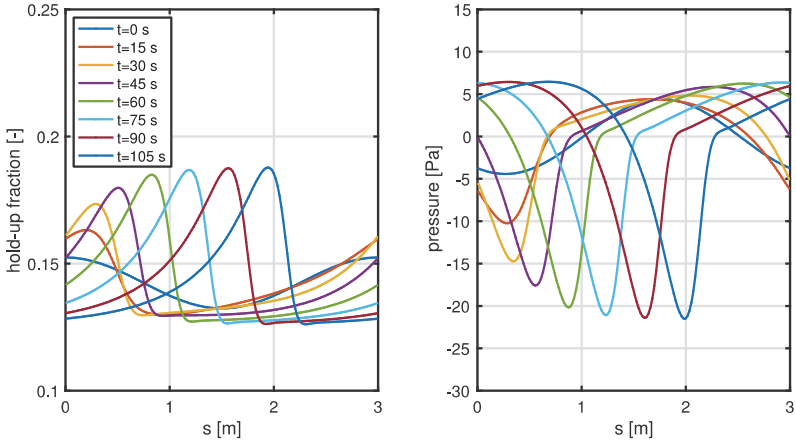

Figure 4: Temporal evolution of roll wave for N=160 in terms of hold-up and deviation from the background pressure. Note that each 15 seconds the roll wave has travelled 10 times through the domain.

Figure 5 shows the roll wave solution at the end of the simulation (t = 200 s) for several grids (shifted such that their maxima are coinciding). It is clear that convergence of the wave shape and pressure profile is obtained upon grid refinement, answering the first question posed in the introduction: *the two-fluid model in four-equation form, discretized with a first-order upwind method is able to capture roll waves, and converged solutions are obtained on fine grids*. On coarse grids the roll wave profiles are smeared out, which is due to the artificial diffusion added by the first order upwind scheme as used in the momentum equation.

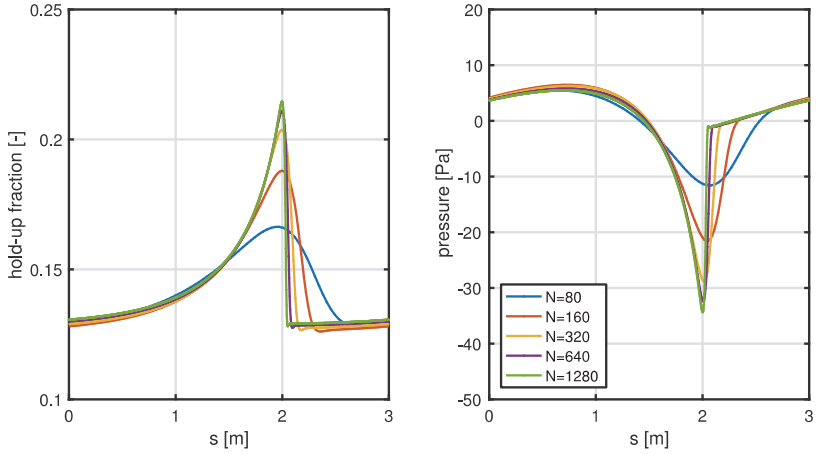

Figure 5: Convergence of wave shape and pressure profile as a function of the number of grid points.

The temporal evolution of the magnitude of the hydraulic jump and of the maximum hold-up level is shown in figure 6. On finer grids, the wave growth is faster, and a steady roll wave solution is obtained earlier in time.

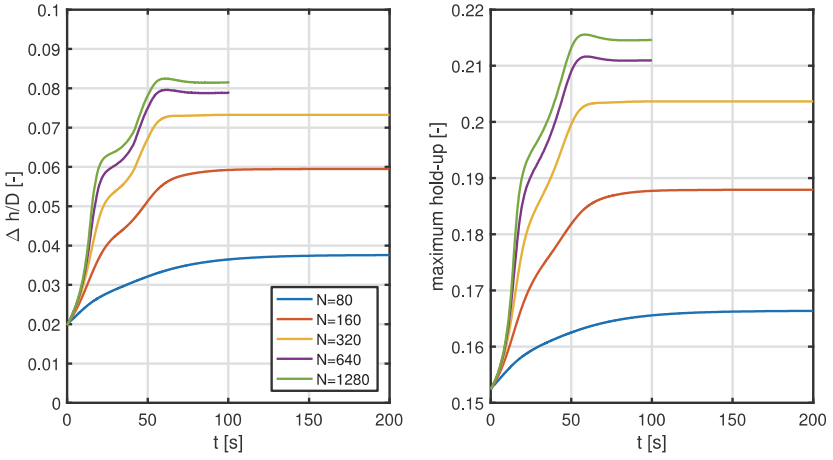

Figure 6: Temporal evolution of hydraulic jump for different grid sizes.

Next, we investigate the convergence of wave speed and jump magnitude towards the analytically predicted values. The wave speed C is computed numerically by tracking the location of maximum hold-up and then computing the derivative by finite differences. The jump magnitude is computed as the difference between the maximum and minimum hold-up values (converted into liquid heights). Interestingly, as can be observed in figure 7, the roll waves do not converge exactly towards the wave speed C and hydraulic jump magnitude Δh as predicted by the analytical solution. The difference is due to the fact that our method is based on the four-equation model, which exhibits different shock solutions than the two-equation model used by Akselsen and Holmås and used to generate the analytical results. This answers the second question posed in the introduction: *the four-equation model shock solutions differ from the two-equation model solutions*. Since the four-equation model is based on the physically conserved quantities, we believe our formulation and corresponding results to be more physical. For the current test case the difference is relatively small, because the shock is rather weak, but in general this will depend on the test case under consideration.

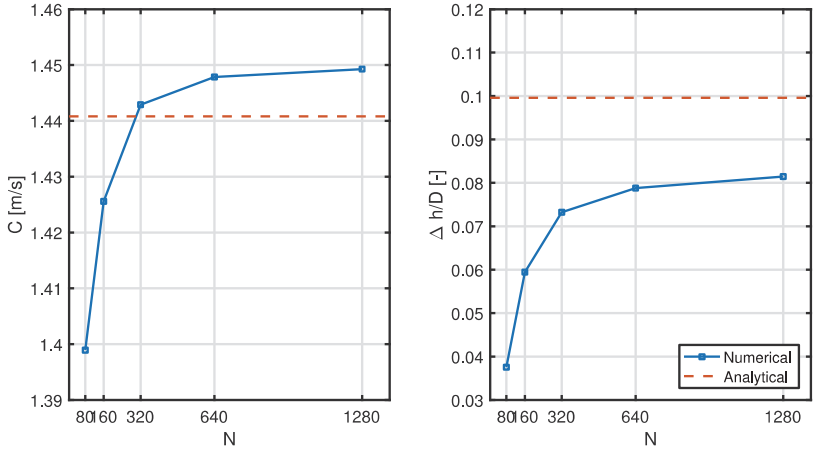

Figure 7: Convergence of wave speed C and jump magnitude $\Delta h / D$ as a function of the number of grid points.

5 CONCLUSION

The questions addressed in this work were whether the two-fluid model in the standard (four equation) form, discretized with a conventional upwind-based finite volume method, is able to capture roll wave solutions, and whether these differ from roll wave solutions obtained with a two-equation model. We have shown that a finite volume discretization of the two-fluid model equations is indeed able to simulate roll waves appearing in multiphase pipelines, and that small differences appear compared to the two-equation model results. We believe our formulation to be more physical, and it has two important advantages compared to existing roll wave simulators described in the literature: (i) it is conservative by construction, meaning that the correct shock magnitude is obtained at the hydraulic jump, and (ii) it can be more easily extended with additional physics (e.g. compressibility, axial diffusion, surface tension), without rederiving the model equations.

The success of performing roll wave simulations with a relatively standard finite volume discretization paves the way for more complex simulations. First, a more accurate (i.e. high order) spatial discretization will reduce the numerical diffusion introduced and will subsequently reduce the number of required grid points. Currently, reasonable results are obtained with 5 grid points per diameter, which can be prohibitive when long pipeline systems are considered. Second, when the superficial velocities are increased, roll waves can transition into slug flow. The behaviour of both the analytical and numerical roll wave model under these conditions, and how to avoid the occurring of ill-posed results, are the next steps in developing accurate slug capturing methods.

ACKNOWLEDGEMENTS

The authors would like to thank Andreas Akselsen for his kind assistance in validating the roll wave solutions.

APPENDIX

The following geometric identities are used to express the wall perimeters, interfacial perimeter, and liquid height in terms of the wetted angle γ_l and pipe diameter $D = 2R$:

$$P_{gl} = D\sin\gamma_l, \tag{28}$$

$$P_l = D\gamma_l, \tag{29}$$

$$P_g = D\left(\pi - \gamma_l\right), \tag{30}$$

$$h = \frac{1}{2}D\left(1 - \cos\gamma_l\right). \tag{31}$$

We use Biberg's approximation [5] to express α_l in terms of γ_l:

$$\gamma_l = \pi\alpha_l + \left(\frac{3\pi}{2}\right)^{\frac{1}{3}}\left(1 - 2\alpha_l + \alpha_l^{\frac{1}{3}} - \alpha_g^{\frac{1}{3}}\right). \tag{32}$$

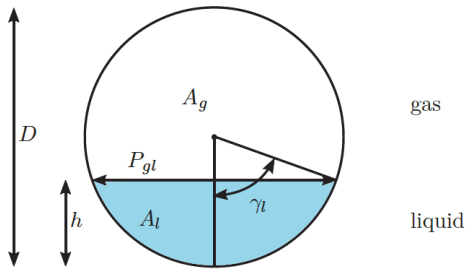

Figure 8: Stratified flow layout and definitions.

REFERENCES

[1] A. H. Akselsen. Efficient Numerical Methods for Waves in One-Dimensional Two-Phase Pipe Flows. PhD thesis, Norwegian University of Science and Technology, 2016.

[2] A. H. Akselsen. Characteristic methods and Roe's method for the incompressible two-fluid model for stratified pipe flow. International Journal of Multiphase Flow, 89:81–91, 2017.

[3] D. Barnea and Y. Taitel. Interfacial and structural stability of separated flow. International Journal of Multiphase Flow, 20:387–414, 1994.

[4] K. Bendiksen, D. Malnes, R. Moe, and S. Nuland. The dynamic two-fluid model OLGA: theory and application. SPE Production Engineering, SPE-19451, 1991.

[5] D. Biberg. An explicit approximation for the wetted angle in two-phase stratified pipe flow. The Canadian Journal of Chemical Engineering, 77(3):1221–1224, 1999.

[6] D. Biberg. A mathematical model for two-phase stratified turbulent duct flow. Multiphase Science and Technology, 19(1):1–48, 2007.

[7] R. Dressler. Mathematical solution of the problem of roll-waves in inclined open channels. Communications on Pure and Applied Mathematics, 2:149–194, 1949.

[8] W. D. Fullmer, V. H. Ransom, and M. A. Lopez De Bertodano. Linear and nonlinear analysis of an unstable, but well-posed, one-dimensional two-fluid model for two-phase flow based on the inviscid Kelvin-Helmholtz instability. Nuclear Engineering and Design, 268(2013):173-184, 2014.

[9] H. Holmås. Numerical simulation of transient roll-waves in two-phase pipe flow. Chemical Engineering Science, 65(5):1811–1825, 2010.

[10] H. Holmås, D. Biberg, G. Johnson, R. Schulkes, and T. Sira. Stability analysis of the Biberg pre-integrated stratified two-phase flow model including profile factors. In 6th North American Conference on Multiphase Technology 6, Banff, Canada, 2008. BHR Group.

[11] R. Issa and M. Kempf. Simulation of slug flow in horizontal and nearly horizontal pipes with the two-fluid model. International Journal of Multiphase Flow, 29(1):69–95, 2003.

[12] G. W. Johnson. A Study of Stratified Gas-Liquid Pipe Flow, PhD thesis, University of Oslo, 2005.

[13] G. W. Johnson, A. F. Bertelsen, and J. Nossen. A mechanistic model for roll waves for two-phase pipe flow. AIChE Journal, 55(11):2788–2795, 2009.

[14] J. Kjølaas, A. De Leebeeck, and S. Johansen. Simulation of hydrodynamic slug flow using the LedaFlow slug capturing model. In 16th International Conference on Multiphase Production Technology, 12-14 June, Cannes, France, 2013.

[15] R. LeVeque. Finite Volume Methods for Hyperbolic Problems, Cambridge University Press, 2002.

[16] R. LeVeque and Z. Li. Immersed interface methods for Stokes flow with elastic boundaries or surface tension. SIAM Journal on Scientific Computing, 18(3):709–735, 1997.

[17] J. Liao, R. Mei, and J. Klausner. A study on the numerical stability of the two-fluid model near ill-posedness. International Journal of Multiphase Flow, 34(11):1067–1087, 2008.

[18] M. López De Bertodano, W. Fullmer, A. Clausse, and V. H. Ransom. Two-Fluid Model Stability, Simulation and Chaos. Springer, 2016.

[19] R. Lyczkowski, D. Gidaspow, C. Solbrig, and E. Hughes. Characteristics and stability analyses of transient one-dimensional two-phase flow equations and their finite difference approximations. Nuclear Science and Engineering, 66(3):378–396, 1978.

[20] B. Sanderse, I. Smith, and M. Hendrix. Analysis of time integration methods for the compressible two-fluid model for pipe flow simulations. International Journal of Multiphase Flow, 95:155–174, 2017.
[21] B. Sanderse and A. E. P. Veldman. Constraint-consistent time-integration methods for one-dimensional incompressible multiphase flow. Submitted to Journal of Computational Physics, 2018.
[22] H. Stewart and B. Wendroff. Two-phase flow: models and methods. Journal of Computational Physics, 56:363–409, 1984.
[23] M. Watson. Wavy stratified flow and the transition to slug flow. In Multi-phase Flow - Proceedings of the 4th International Conference, pages 495–512, 1989.